



# Porcine Gasdermin D Is a Substrate of Caspase-1 and an Executioner of Pyroptosis

Yueyang Song<sup>1,2</sup>, Jiameng Song<sup>1,2</sup>, Meng Wang<sup>1,2</sup>, Junwei Wang<sup>1,2</sup>, Bo Ma<sup>1,2\*</sup> and Wenlong Zhang<sup>1,2\*</sup>

<sup>1</sup> College of Veterinary Medicine, Northeast Agricultural University, Harbin, China, <sup>2</sup> Northeastern Science Inspection Station, China Ministry of Agriculture Key Laboratory of Animal Pathogen Biology, Harbin, China

## OPEN ACCESS

### Edited by:

Christine A. Jansen,  
Wageningen University and Research,  
Netherlands

### Reviewed by:

Parimal Samir,  
St. Jude Children's Research Hospital,  
United States  
Marcin Poreba,  
Wrocław University of Science and  
Technology, Poland

### \*Correspondence:

Wenlong Zhang  
zhangwenlong@neau.edu.cn  
Bo Ma  
mabo99@neau.edu.cn

### Specialty section:

This article was submitted to  
Comparative Immunology,  
a section of the journal  
Frontiers in Immunology

**Received:** 04 December 2021

**Accepted:** 16 February 2022

**Published:** 14 March 2022

### Citation:

Song Y, Song J, Wang M, Wang J,  
Ma B and Zhang W (2022) Porcine  
Gasdermin D Is a Substrate  
of Caspase-1 and an  
Executioner of Pyroptosis.  
*Front. Immunol.* 13:828911.  
doi: 10.3389/fimmu.2022.828911

Gasdermin (GSDM) family proteins were recently identified as the executioner of pyroptosis. The mechanism of pyroptosis mediated by gasdermin D (GSDMD) (a member of GSDM family) in humans and mice is well understood. In pyroptosis, mouse and human GSDMDs are cleaved by activated proinflammatory caspases (caspase-1, 4, 5, or 11) to produce amino-terminal domain (GSDMD-NT) and a carboxyl-terminal domain (GSDMD-CT). The GSDMD-NT drives cell membrane rupture, which leads to the pyroptotic death of the cells. The expression of porcine GSDMD (pGSDMD) has recently been determined, but the activation and regulation mechanism of pGSDMD and its ability to mediate pyroptosis are largely unknown. In the present study, the activation of porcine caspase-1 (pcaspase-1) and cleavage of pGSDMD occurred in the duodenum and jejunum of a piglet challenged with enterotoxigenic *Escherichia coli* were first determined. Then the capability of pcaspase-1 to cleave pGSDMD was determined in a cell-free system and in human embryonic kidney cells. The pGSDMD cleavage by pcaspase-1 occurred after the pGSDMD molecule's <sup>276</sup>Phenylalanine-Glutamine-Serine-Aspartic acid<sub>279</sub> motif. The pGSDMD-NT generated from the pGSDMD cleavage by pcaspase-1 showed the ability to drive cell membrane rupture in eukaryotic cells. When expressed in *E. coli* competent cells, pGSDMD-NT showed bactericidal activity. These results suggest that pGSDMD is a substrate of pcaspase-1 and an executioner of pyroptosis. Our work sheds light on pGSDMD's activation mechanisms and functions.

**Keywords:** porcine GSDMD, porcine caspase-1, cleavage, substrate, pyroptosis

## INTRODUCTION

Pyroptosis is a type of programmed cell death (1) that is characterized by cell swelling, breakdown of the plasma membrane, release of cytoplasmic contents, and vigorous inflammatory immune responses. Pyroptosis has been proven to be closely related to various human diseases, including infectious (2–4) and non-infectious diseases (5–7).

Members of gasdermin (GSDM) family have recently been proven as the executioners of pyroptosis (8–10). Gasdermin A (GSDMA), GSDMB, GSDMC, GSDMD, GSDME (also known as deafness, autosomal dominant 5, DFNA5), and DFNB59 are the six GSDMs that have been

identified in humans (11, 12). GSDMD is the most widely studied GSDM protein in humans and mice. The cleavage of GSDMD by human and mouse caspase-1 or by human caspase-4/5/8 and mouse caspase-8/11 is the critical event of pyroptosis (8, 13, 14). The amino-terminal domain of GSDMD (GSDMD-NT), one of the caspase cleavage products, oligomerizes and forms pores in the plasma membrane, leading to pyroptotic cell death and thereby causes the release of proinflammatory cell components (15, 16).

In contrast with the extensive research on GSDM-mediated pyroptosis in humans and mice, research on the underlying mechanisms of cell pyroptosis in other species, such as pigs, is limited. An early study determined that *Salmonella typhimurium* infection increased caspase-1 expression to induce pyroptosis in porcine mesenteric lymph nodes (17). A recent study found that pathogenic *Escherichia coli* (*E. coli*) induced the upregulation of mRNA levels of NOD-like receptor (NLR) family, pyrin domain-containing protein 3 (NLRP3), apoptosis-associated speck-like protein containing CARD (ASC), caspase-1, IL-1 $\beta$ , IL-18, and GSDMD in infected pigs (18). Another recent work reported that classical swine fever virus (CSFV) infection activates caspase-1 and promotes GSDMD cleavage to produce GSDMD-NT in the peripheral immune organs of pigs and porcine peripheral blood monocytes (19, 20). Transmissible gastroenteritis virus (TGEV) has been reported to cause caspase-1 activation and GSDMD cleavage in porcine intestinal epithelial cells (21). These studies seemingly provide an explanation for the mechanism of cell pyroptosis in pigs. However, first, these studies enrolled human or mice GSDMD-specific antibodies as research tools, which creates doubt on whether their findings accurately reflect the cleavage of porcine GSDMD (pGSDMD). Second, if the GSDMD cleavage, which had been observed in these studies, indeed occurred, then whether a direct relationship exists between caspase-1 activation and GSDMD cleavage is unclear. Third,

whether the cleavage products of pGSDMD can cause pyroptotic cell death remains unclear. The pyroptosis in pig thus deserves a separate research.

In the current study, we used self-prepared pGSDMD and porcine caspase-1 (pcaspase-1)-specific antibody and found that pcaspase-1 activation and pGSDMD cleavage occurred in the small intestine of a piglet challenged with enterotoxigenic *E. coli* (ETEC). We then found that pcaspase-1 can cleave pGSDMD between Aspartic acid (D)279 and Glycine (G)280. The pGSDMD-NT demonstrates the ability to cause pyroptosis in different cells lines and bactericidal activity. Our work sheds light on pGSDMD's activation mechanisms and functions.

## MATERIALS AND METHODS

### Plasmids and Antibodies

First, pUC57-pcaspase-1, a plasmid that contain the full-length porcine caspase-1 gene (GenBank Accession No.AB027296), was synthesized and constructed by GenScript (Nanjing, China). pET-30a(+)-His-pGSDMD, a plasmid that contains the full-length pGSDMD gene, was previously constructed in our laboratory (22).

The eukaryotic and prokaryotic expression plasmids that contain the nucleic acids encoding full-length/truncated pGSDMD or pcaspase-1 were constructed *via* standard PCR cloning strategy using the primers listed in **Table 1**. A prokaryotic expression plasmid that contains the nucleic acid encoding a mutant of pGSDMD was constructed from the pET-30a(+)-His-pGSDMD plasmid using the primers listed in **Table 1** and QuickMutation™ Site-Directed Mutagenesis Kit (Beyotime, Beijing, China) according to the manufacturer's instructions. All recombinant plasmids were verified by DNA sequencing. The resulting constructions mentioned above are listed in **Table 2**.

**TABLE 1** | Primers used for plasmid construction.

| Name of plasmids            | Nucleotide of primer (5' to 3')  | Restrict sites                  |
|-----------------------------|--|---------------------------------|
| pET-30a(+)-pcaspase-1 p20   | <u>GAAGATCTGGACGACGACGACAAGAACCCAGTTAAGCCTG</u><br><u>CCGGAATTC</u> TTAATCTTTATCCATACG | <i>Bgl</i> II<br><i>Eco</i> R I |
| pET-30a(+)-His-pcaspase-1   | <u>CCGGAATTC</u> ATGGCCGATAAGGTGC<br><u>CGGCTCGAG</u> TTAATGTCTGGGAAG                  | <i>Eco</i> R I<br><i>Xho</i> I  |
| pET-30a(+)-pcaspase-1-His   | <u>CGCCATATGGCCGATAAGGTGCTG</u><br><u>CGGCTCGAG</u> ATGTCTGGGAAGAG                     | <i>Nde</i> I<br><i>Xho</i> I    |
| pET-30a(+)-Apcaspase-1-His  | <u>CGCCATATGAACCCAGTTAAGCCTG</u><br><u>CGGCTCGAG</u> ATGTCTGGGAAGAG                    | <i>Nde</i> I<br><i>Xho</i> I    |
| pcDNA3.1(+)-pcaspase-1 p20  | <u>CCGGAATTC</u> ACCATGGCTAACCCAGTTAAGCC<br><u>CGGCTCGAG</u> TTAATCTTTATCCATACG        | <i>Eco</i> R I<br><i>Xho</i> I  |
| pEGFP-C1-pGSDMD             | <u>CCGGAATTC</u> GATGGCATCAGCCTTTGAG<br><u>GCTCTAGACTAGCAGAGCTGGCTGAG</u>              | <i>Eco</i> R I<br><i>Xba</i> I  |
| pET-30a(+)-His-pGSDMD-NT    | <u>CCGGAATTC</u> ATGGCATCAGCCTTTGAG<br><u>ACGCGTCCGACTT</u> AGTCTGACTGGAACTTCAG        | <i>Eco</i> R I<br><i>Sal</i> I  |
| pET-30a(+)-His-pGSDMD-CT    | <u>CCGGAATTC</u> ATGGGGCCCGCGGAGGACCAG<br><u>ACGCGTCCGACCT</u> AGCAGAGCTGGCTGAG        | <i>Eco</i> R I<br><i>Sal</i> I  |
| pcDNA3.1(+)-pGSDMD-CT       | <u>CCGGAATTC</u> ATGGGGCCCGCGGAGGACCAG<br><u>GCTCTAGACTAGCAGAGCTGGCTGAG</u>            | <i>Eco</i> R I<br><i>Xba</i> I  |
| pET-30a(+)-His-pGSDMD D279A | <u>CTGAAGTCCAGT</u> CAGCCGGGCCCGCGGAGG<br><u>GACTTCAAGTCA</u> GTCGGCCCGGGCGCCTCC       |                                 |

Restriction enzyme recognition sites are underlined in each sequence and listed in the right column.

**TABLE 2** | Plasmids used in experiments.

| Name of plasmids            | Details  |
|-----------------------------|--|
| pUC57-pcaspase-1            | Stored in our laboratory   |
| pUC57-pGSDMD                | Stored in our laboratory   |
| pET-30a(+)-pcaspase-1 p20   | Prepared by this study, encoding 120-297aa of pcaspase-1 with a N-terminal 6×His tag                           |
| pET-30a(+)-His-pcaspase-1   | Prepared by this study, encoding full-length pcaspase-1 with a N-terminal 6×His tag                            |
| pET-30a(+)-pcaspase-1-His   | Prepared by this study, encoding full-length pcaspase-1 with a C-terminal 6×His tag                            |
| pET-30a(+)-Δpcaspase-1-His  | Prepared by this study, encoding pcaspase-1 without the 1-120aa prodomain and with a C-terminal 6×His tag      |
| pcDNA3.1(+)-pcaspase-1      | Prepared by this study, encoding full-length pcaspase-1  |
| pEGFP-C1-pGSDMD             | Prepared by this study, encoding full-length pGSDMD with a N-terminal fused enhanced green fluorescent protein |
| pET-30a(+)-His-pGSDMD D279A | Prepared by this study, encoding a pGSDMD mutant of which the aspartate (D)279 is replaced with an alanine (A) |
| pET-30a(+)-His-pGSDMD-CT    | Prepared by this study, encoding 280-489aa of pGSDMD with a N-terminal 6×His tag                               |
| pcDNA3.1(+)-pGSDMD-CT       | Prepared by this study, encoding 280-489aa of pGSDMD   |
| pET-30a(+)-His-pGSDMD-NT    | Prepared by our laboratory, encoding 1-279aa of pGSDMD with a N-terminal 6×His tag                             |
| pcDNA3.1(+)-pGSDMD-NT       | Prepared by our laboratory, encoding 1-279aa of pGSDMD   |
| pET-30a(+)-His-pGSDMD       | Prepared by our laboratory, encoding full-length pGSDMD with a N-terminal 6×His tag                            |
| pcDNA3.1(+)-pGSDMD          | Prepared by our laboratory, encoding full-length pGSDMD  |

A mouse monoclonal antibody recognizing the C-terminal domain of pGSDMD was generated in our laboratory (the process for preparing the monoclonal antibody is described in detail in another manuscript currently under review). The mouse monoclonal antibody against the p20 subunit of pcaspase-1 was generated using the prokaryotically expressed and purified recombinant pcaspase-1p20. Anti-β-actin (2P2) mouse mAb (M20011, Abmart), mouse anti-His tag mAb (TA-02, ZSGB-BIO), horseradish peroxidase (HRP)-conjugated goat anti-mouse IgG (H+L) (ZB-2305, ZSGB-BIO), and HRP-conjugated goat anti-rabbit IgG (H+L) (ZB-2301, ZSGB-BIO) were commercially available.

## Piglet Tissue and Protein Extraction

The tissues of piglets, which had been orally challenged with ETEC (F5+), were provided by Dr. Ping Zhang, Northeast Agricultural University. The tissues were cut into small pieces and then frozen in liquid nitrogen. The frozen tissues were ground into powder. The powder was suspended in RIPA buffer (supplied with 1% PMSF) and placed on ice for 10 min. The mixtures were centrifuged at 12,000 × g for 15 min at 4°C, and the supernatant was collected and subjected to Western blot analysis.

## Cell Culture

Human embryonic kidney (HEK293) cells, intestinal porcine enterocytes (IPEC-J2), and Madin–Darby bovine kidney (MDBK) cells were cultured in Dulbecco's Modified Eagle's Medium (GIBCO, Shanghai, China) supplemented with 10% fetal bovine serum (FBS) (ABW, Shanghai, China). Mouse fibroblast cells (L929) were cultured in RPMI medium 1640 (GIBCO, Shanghai, China) containing 10% FBS. Cells were all incubated at 37°C in a 5% CO<sub>2</sub> incubator.

## Transfection and Drug Treatment

For transfection, HEK293 cells were seeded into six-well cell culture plates at a density of 2 × 10<sup>5</sup> cells. The cells were grown at 37°C overnight and then transfected with different plasmids, as indicated in the Results section, using a polyethylenimine linear transfection reagent (BIOHUB, Shanghai, China) according to the manufacturer's instructions. For inhibition experiments,

Z-VAD-FMK (A1902, APEX-BIO) or VX-765 (A8238, APEX-BIO) was added to the cells 4 h after transfection. The cells were harvested at the indicated time points and lysed in RIPA buffer (supplied with 1% PMSF) on ice for 10 min. The mixtures were centrifuged at 12,000 × g for 15 min at 4°C, and the supernatant was collected and subjected to Western blot analysis.

## Lactate Dehydrogenase Assay

HEK293, IPEC-J2, L929, and MDBK cells were seeded in 24-well plates at a density of 1.5 × 10<sup>5</sup> cells/well. After an overnight growth, the cells were transfected with either pcDNA3.1 (+)-pGSDMD (1 μg/well), pcDNA3.1(+)-pGSDMD-NT (1 μg/well), or pcDNA3.1(+)-pGSDMD-CT (1 μg/well). At the indicated time points after transfection, lactate dehydrogenase (LDH) activity in the culture supernatants was measured using an LDH Cytotoxicity Assay Kit (Beyotime, Beijing, China) following the manufacturer's instruction.

## Microscope Observation

To determine the morphological change of transfected cells, cells were observed under an inverted microscope, and the static bright-field cell images were captured. Propidium iodide at 1 μg/mL (Beyotime, Beijing, China) was added concurrently for imaging experiments.

## Preparation of Recombinant pGSDMD (His-rpGSDMD) and His-rpGSDMD D279A

His-rpGSDMD was prokaryotically expressed and purified as described in a previous study (22). His-rpGSDMD D279A was prepared following the same protocol.

## Preparation of Activate rpcaspase-1

To obtain the active form of rpcaspase-1, pET-30a(+)-His-pcaspase-1, pET-30a(+)-pcaspase-1-His, and pET-30a(+)-Δpcaspase-1-His were transformed into *E. coli* Rosetta (DE3)<sup>TM</sup>. Recombinant proteins were expressed by inducing with 0.2 mM IPTG at 25°C for 4 h and shaking at 220 r/min. The bacteria were harvested by centrifuging at 5,000 × g at 4°C for 15 min and washed twice with ice-cold phosphate buffered solution (PBS). The bacteria were finally resuspended in PBS and

lysed by sonication. The expression and autoprocessing of rpcaspase-1 in *E. coli* were analyzed by sodium dodecyl sulfate-polyacrylamide gel electrophoresis (SDS-PAGE) and visualized through Western blot analysis using mouse anti-rpcaspase-1 p20 mAb. The supernatant of bacteria lysate was collected after centrifugation at 12,000 ×g at 4°C for 15 min. The rpcaspase-1 activity was determined using Ac-YVAD-pNA (chromogenic substrate of caspase-1) (P9701, Beyotime). Briefly, 89 μL of the supernatant of bacteria lysate was mixed with 10 μL 10×reaction buffer (0.5 M HEPES [pH 7.5], 30 mM EDTA, 1.5 M NaCl, 0.05% [v/v] Tween 20, and 0.1 M DTT) and 1 μL Ac-YVAD-pNA solution (20 mM). The mixtures were incubated at 37°C for 7 h. Absorbance was measured at 405 nm at one-hour intervals. The experiment was performed in triplicate.

### In Vitro Cleavage Assay

First, 40 μL of purified His-rpGSDMD and His-rpGSDMD D279A (8 μg in total) was mixed, respectively, with different volumes of the supernatant of the *E. coli* lysate that showed caspase-1 activity and 10 μL 10× reaction buffer. PBS was added to the mixtures to a final volume of 100 μL. The mixtures were incubated at 37°C for different periods. The cleavage of His-rpGSDMD by His-rpcaspase-1 was analyzed by SDS-PAGE and visualized through Western blot analysis.

The ability of rpcaspase-3-His in cleaving His-rpGSDMD was also tested and analyzed by SDS-PAGE and Western blot assay.

Z-VAD-FMK (A1902, APExBIO), VX-765 (A8238, APExBIO), or Z-DEVD-FMK (caspase-3 inhibitor) (A1920, APExBIO) was used in several experiments to determine the specificity of His-rpcaspase-1 and rpcaspase-3-His in cleaving His-rpGSDMD.

### Bactericidal Assay

*E. coli* Rosetta (DE3)<sup>TM</sup> was transformed with pET-30a(+) expressing pGSDMD, pGSDMD-NT, or pGSDMD-CT. The transformants were cultured in LB medium containing 30 μg/mL kanamycin (Kan) at 37°C to OD<sub>600nm</sub> that reached 0.6–0.8. Bacteria cells were diluted and grown on LB agar plates containing 30 μg/mL Kan and with or without 0.5 mM IPTG. After incubation at 37°C overnight, colony forming units on the plates were counted and statistically calculated.

In another independent experiment, *E. coli* transformants were cultured in LB medium containing 30 μg/mL Kan at 37°C to OD<sub>600nm</sub> that reached 0.6–0.8. Next, IPTG was added into the medium. The cultures were further incubated at 37°C for 6 h. The OD<sub>600nm</sub> value of the cultures were detected at one-hour intervals.

### Western Blot Assay

The protein concentration in samples was quantified using BCA protein assay kit (P0012, Beyotime). Proteins were then subjected to SDS-PAGE and transferred to nitrocellulose membranes. The membranes were blocked with 5% skim milk in PBS plus 0.05% (v/v) Tween 20 (PBST) at room temperature for 1 h. The membranes were then incubated with any of the mouse anti-rpGSDMD mAb (1:2,000), mouse anti-rpcaspase-1 p20 mAb, anti-β-actin (2P2) mouse mAb (1:5,000), and mouse anti-His tag

mAb (1:5,000) at 4°C overnight and then incubated with HRP-conjugated goat anti-mouse IgG(H+L)(1:5,000) at room temperature for 1 h. Membranes were washed thrice with PBST for 5 min after each incubation step. Detection was conducted using BeyoECL Star (Beyotime, Beijing, China) following the manufacturer's instructions.

### Statistical Analysis

Statistical analysis was conducted using GraphPad Prism 8 software, and all experiments were performed in triplicate. The two-sample student *t* test and one-way ANOVA was used for comparisons between groups. A *p* value < 0.05 was considered statistically significant.

## RESULTS

### Activation of pcaspase-1 and Cleavage of pGSDMD in ETEC (F5+) Challenged Piglet

The protein samples of the heart, liver, spleen, lung, kidney, duodenum, and jejunum of a piglet challenged with ETEC (F5+) were analyzed by Western blot assay. The results show that pcaspase-1 p20 and pGSDMD-CT can be detected in the duodenum and jejunum of the piglet but not in the other five organs (Figure 1A). The results also indicate that the activation of pcaspase-1 and the cleavage of pGSDMD in the piglet occurred simultaneously. The pcaspase-1 activation and pGSDMD cleavage occurred in the jejunum of the piglet challenged with ETEC (F5+) but not in the jejunum of the healthy piglet (Figure 1B). Considering that the pcaspase-1 activation and the pGSDMD cleavage are consistent in the tissue distribution, we speculate that pcaspase-1 activation and pGSDMD cleavage are closely associated.

### Preparation of Active rpcaspase-1

To obtain the active rpcaspase-1, three strategies were adopted (Figure 2A). The SDS-PAGE showed that only the Δrpcaspase-1-His was highly expressed in *E. coli*. By contrast, the expression of His-rpcaspase-1 and rpcaspase-1-His could not be determined by SDS-PAGE due to the poor expression efficiency (Figure 2A). Western blot assays were hence performed. The results show that p20 subunit can only be detected in *E. coli* that expressed the His-rpcaspase-1 by mouse anti-pcaspase-1 p20 monoclonal antibody (Figure 2A).

The enzymatic activity of rpcaspase-1 in pET-30a(+)-His-pcaspase-1 and pET-30a(+)-pcaspase-1-His transformed *E. coli* was then examined by using caspase-1 substrate (Ac-YVAD-pNA). The results show that His-rpcaspase-1 can cleave Ac-YVAD-pNA, but rpcaspase-1-His did not display any caspase activity (Figure 2B). The cleavage of Ac-YVAD-pNA by His-rpcaspase-1 reached its peak within 3 h, because the OD<sub>405nm</sub> value of the reaction mixture did not increase after 3 h. The His-rpcaspase-1 was not purified for two reasons. First, the expression level of the His-rpcaspase-1 was extremely low. Second, the His-CARD region of the His-rpcaspase-1 was removed in the self-activation process.

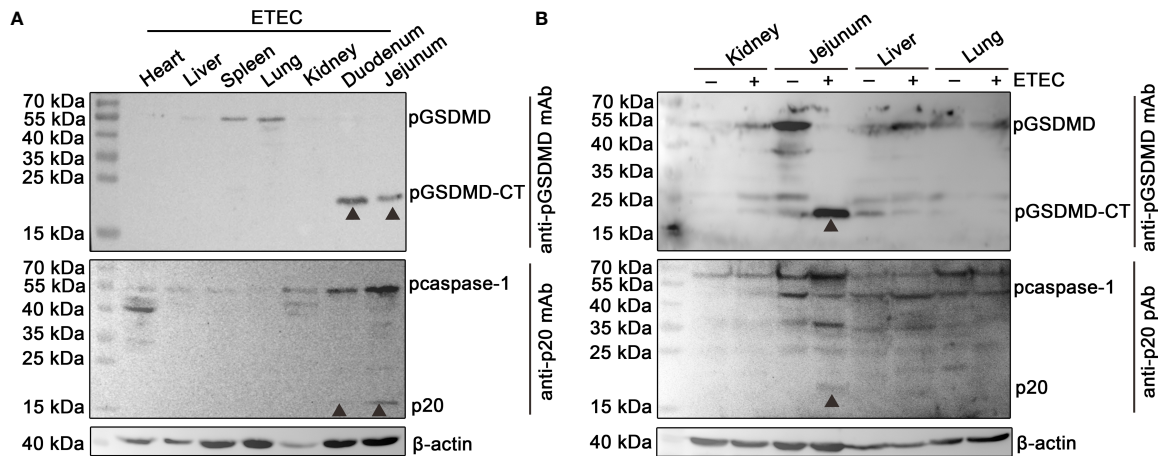


**FIGURE 1** | Determination of the activation of pcaspase-1 and cleavage of pGSDMD in tissues of the piglet. **(A)** Determination of the activation of pcaspase-1 and cleavage of pGSDMD in the tissues of ETEC (F5+) challenged piglet. The heart, liver, spleen, lung, kidney, duodenum and jejunum of a piglet orally challenged with  $1 \times 10^{11}$  CFU of ETEC (F5+). **(B)** Difference in pcaspase-1 activation and pGSDMD cleavage in tissues between the healthy and ETEC (F5+) challenged piglets. The activation of pcaspase-1 and cleavage of pGSDMD in the kidneys, jejunums, livers and lungs of the piglets were analyzed by western blot assay. GSDMD: full-length GSDMD; GSDMD-CT: C-terminal cleavage product of GSDMD; p20: mature caspase-1.

## pGSDMD Is a Substrate of pcaspase-1

His-rpGSDMD was incubated with the supernatant of the *E. coli* lysate that contains active His-rpcaspase-1. The cleavage of His-rpGSDMD was determined by Western blot assays using anti-His tag monoclonal antibody and anti-pGSDMD monoclonal antibody as the primary antibodies. The results reveal that two proteins with molecular weights of approximately 40 kDa and 20 kDa can be recognized by anti-His tag monoclonal antibody and anti-pGSDMD monoclonal antibody, respectively (Figure 3A). The molecular weights of the two proteins are inconsistent with the predicted caspase-1 cleavage products of the His-rpGSDMD (a 38-kDa rpGSDMD-NT fragment involving a 7-kDa His-tag) and a 22-kDa rpGSDMD-CT fragment. The two protein fragments were not detected in mixtures of His-rpGSDMD and the supernatant of the *E. coli* lysate transformed with pET-30a(+) (Figure 3A).

To determine whether pcaspase-1 can cleave pGSDMD in eukaryocytes, HEK293 cells were co-transfected with pEGFP-C1-pGSDMD and pcDNA3.1(+)-pcaspase-1 for 48 h. A protein with a molecular weight similar to that of the predicted pGSDMD-CT was detected (Figure 3B). This protein was not detected in control cells and cells transfected with the plasmids, as indicated in Figure 3B. The results of LDH release assay show that the cells co-transfected with pcDNA3.1(+)-pcaspase-1 and pEGFP-C1-pGSDMD released more LDH than cells transfected with pcDNA3.1(+)-pcaspase-1 or pEGFP-C1-pGSDMD and control cells (Figure 3C).

These results indicate that pGSDMD may be a substrate of pcaspase-1 and that the cleavage products can cause cell membrane damage.

## Caspase Inhibitors Abolished the Cleavage of pGSDMD by pcaspase-1

To determine whether the enzymatic activity of the recombinantly expressed pcaspase-1 is necessary for pGSDMD cleavage, cleavage

assays were performed in the presence of VX-765 (a caspase-1 inhibitor) and Z-VAD-FMK (a pan-caspase inhibitor). The results show that both VX-765 and Z-VAD-FMK inhibited the pGSDMD cleavage in the cell-free system (Figures 4A, B) and HEK293 cells in a dose-dependent manner (Figures 4C, D). The results indicate that the enzymatic activity of pcaspase-1 is required for pGSDMD cleavage.

## D279 Is Essential for pGSDMD Cleavage by pcaspase-1

On the basis of previous reports (8, 23), we speculated that the recognition motif of pcaspase-1 in pGSDMD is  $_{276}$ Phenylalanine-Glutamine-Serine-Aspartic acid $_{279}$  ( $_{276}$ FQSD $_{279}$ ). We then generated and prepared a mutant of pGSDMD (named His-rpGSDMD D279A), of which the D279 was replaced with an alanine (A) (Figure 5A). As expected, the D279A mutation completely abolished the cleavage of His-rpGSDMD by His-rpcaspase-1 (Figure 5B). The result confirms that the D279 in pGSDMD molecule is essential for its cleavage by pcaspase-1.

## pGSDMD-NT Causes Cell Membrane Damage

To determine the effect of pGSDMD-NT on the cell membrane's integrity, pcDNA3.1(+)-pGSDMD-NT was transfected into IPEC-J2, HEK293, L929, and MDBK cells. The LDH release of the cells was measured. The results show that the cells transfected with pcDNA3.1(+)-pGSDMD-NT released more LDH than cells transfected with pcDNA3.1(+)-pGSDMD-CT, pcDNA3.1(+)-pGSDMD or pcDNA3.1(+) and control cells (Figure 6A).

In contrast to pGSDMD-CT and full-length pGSDMD, pGSDMD-NT could cause extensive cell death in HEK293 cells with apparent pyroptosis morphology (Figure 6B). The results of PI



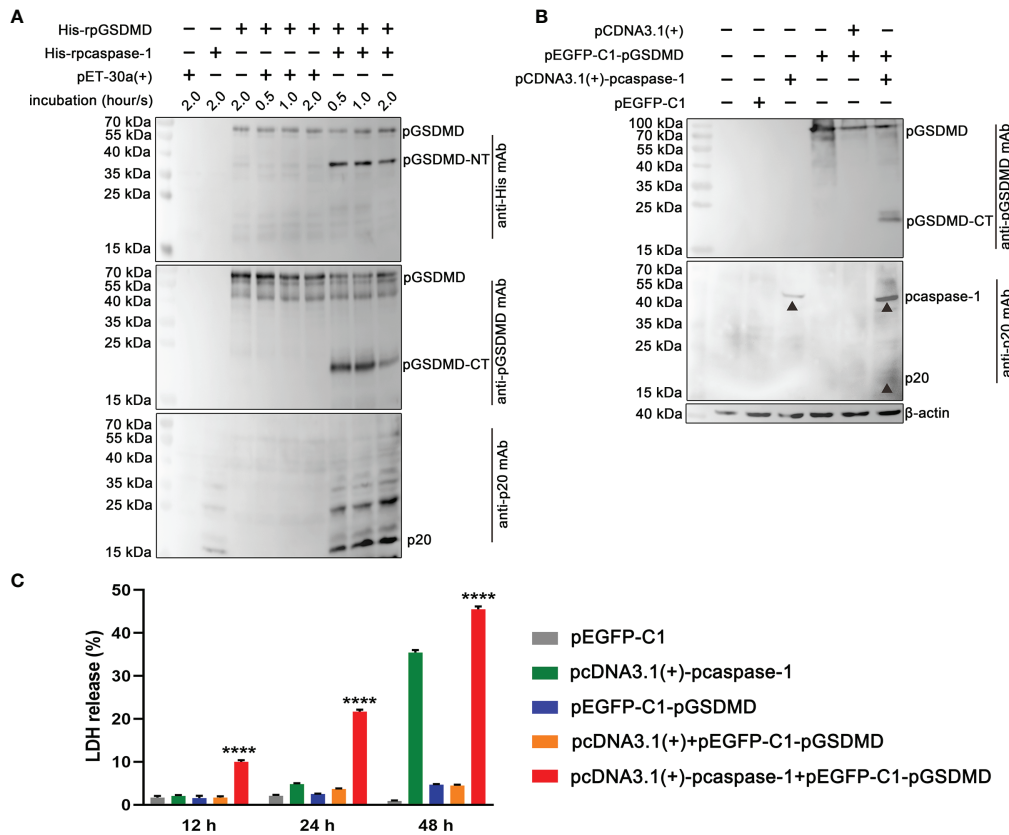


**FIGURE 3** | *In vitro* cleavage of pGSDMD by pcaspase-1. **(A)** Cleavage of His-rpGSDMD by His-rpcaspase-1 in a cell-free system. Purified His-rpGSDMD was incubated with *E. coli* lysate containing His-rpcaspase-1 for 0.5, 1 and 2 h. The products were analyzed by western blot assays using mouse Anti-His mAb, mouse anti-rpGSDMD mAb and mouse anti-rpcaspase-1 p20 mAb. The mixtures of His-rpGSDMD and the cell lysate of pET30a(+) transformed *E. coli* were used as controls. **(B)** Cleavage of pGSDMD by pcaspase-1 in HEK293 cells. HEK293 cells were transfected pEGFP-C1-pGSDMD and pcDNA3.1(+)-pcaspase-1 simultaneously. The Cells transfected with either of the two plasmids and the cells co-transfected with pEGFP-C1-pGSDMD and pcDNA3.1(+) served as controls. 48 h after the transfection, whole cell lysates were analyzed by mouse anti-rpGSDMD mAb. **(C)** Determination of the cellular LDH release of the transfected cells. The supernatant of the transfected HEK293 cells was collected 12, 24 and 48 h after the transfection and the LDH release of the cells was measured. Values are the means of triplicates and shown as means ± SD. \*\*\*\**p* < 0.0001. GSDMD, full-length GSDMD; GSDMD-NT, N-terminal cleavage product of GSDMD; GSDMD-CT, C-terminal cleavage product of GSDMD; p20, mature caspase-1.

cleavage of His-rpGSDMD is indeed mediated by rpcaspase-3-His. By analyzing the pGSDMD’s primary structure, we found a motif that can be recognized by caspase-3, located at the 84aa to 87aa positions of the pGSDMD molecule (**Figure 8C**). The molecular weights of the two predicted cleavage products are approximately 8 kDa and 43 kDa, respectively. The predicted large cleavage product involves the pGSDMD-CT. The characteristics of the predicted large cleavage product are consistent with the 40-kDa protein observed on the gel and blot. Therefore, we speculate that the pcaspase-3 can cleave the pGSDMD between D87 and G88.

## DISCUSSION

Although previous studies have shown that pGSDMD is cleaved when porcine cells are infected with different pathogens (19–21),

how pGSDMD is cleaved and the effect of pGSDMD cleavage on the fate of cells remain unclear. A recent work showed that Seneca Valley Virus 3C protease can cleave pGSDMD after the glutamine 193 and glutamine 277 (23). As far as we know, the above study is a pilot research on the cleavage mechanism of pGSDMD. However, from the host’s perspective, the underlying mechanism of pGSDMD cleavage remains unknown.

In the present study, we first determined that the pcaspase-1 activation and the pGSDMD cleavage occurred in the small intestinal tissue of a piglet challenged with ETEC (F5+) (**Figure 1**). To our best knowledge, the present work is the first investigation that uses a pGSDMD-specific monoclonal antibody as a research tool. A previous study showed that CSFV infection caused the pcaspase-1 activation and the pGSDMD cleavage in peripheral lymphoid organs of infected pigs (19). These results indicated that the pcaspase-1 activation and the pGSDMD cleavage generally have a similar tissue distribution pattern in pigs. Considering that GSDMD is mainly cleaved by caspase-1 in

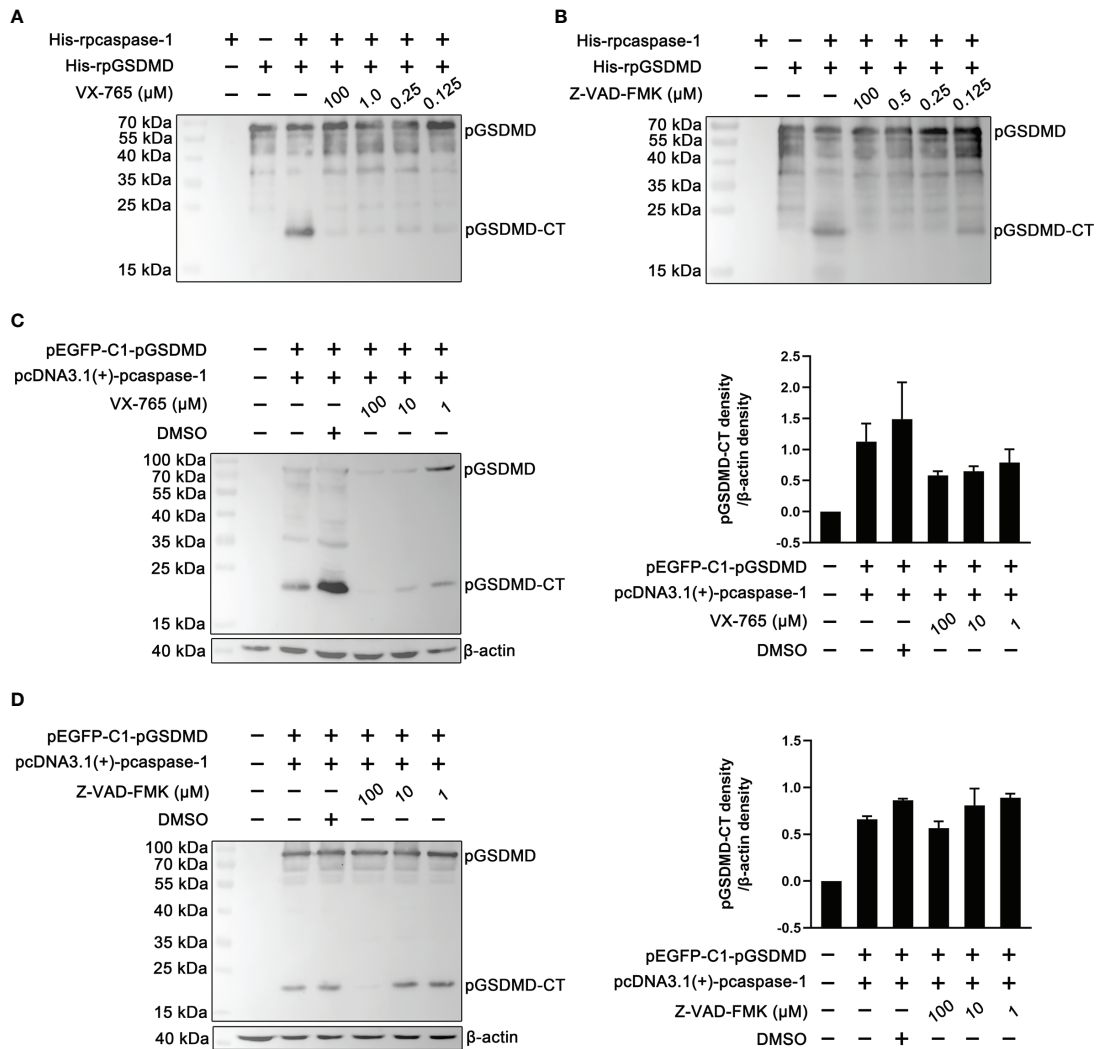


**FIGURE 4** | The effect of VX-765 and Z-VAD-FMK on the cleavage of pGSDMD by pcaspase-1. His-rpGSDMD was incubated with His-rpcaspase-1 in the presence of VX-765 (A) or Z-VAD-FMK (B), the mixtures were analyzed by western blot analysis using mouse anti-rpGSDMD mAb. HEK293 cells were transfected with pEGFP-C1-pGSDMD and pcDNA3.1(+)-pcaspase-1 simultaneously, and then, VX-765 (C) or Z-VAD-FMK (D) were used to treat the cells for 18 h. The whole cell lysates were analyzed by mouse anti-rpGSDMD mAb based western blot assay (left panel). The density of pGSDMD-CT bands was quantified using the ImageJ software and normalized to β-actin (right panel).

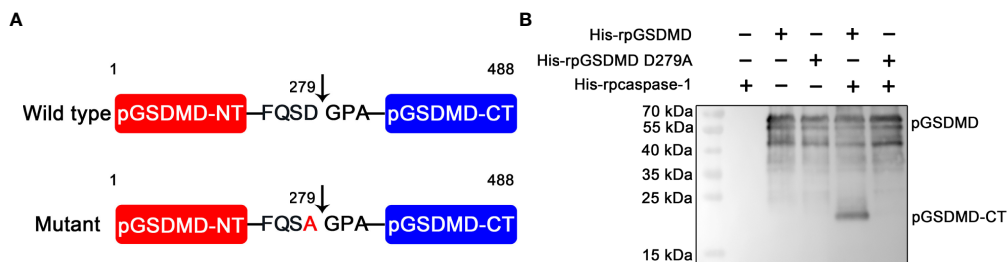


**FIGURE 5** | D279A mutation abolished the cleavage of His-rpGSDMD by His-rpcaspase-1. (A) The diagram of deduced cleavage site of pcaspase-1 in pGSDMD. The D279 was replaced with an alanine in the His-rpGSDMD D279A mutant. (B) His-rpGSDMD D279A and His-rpGSDMD were incubated with His-rpcaspase-1, respectively. The products were analyzed by Western blot analysis using mouse anti-rpGSDMD mAb.

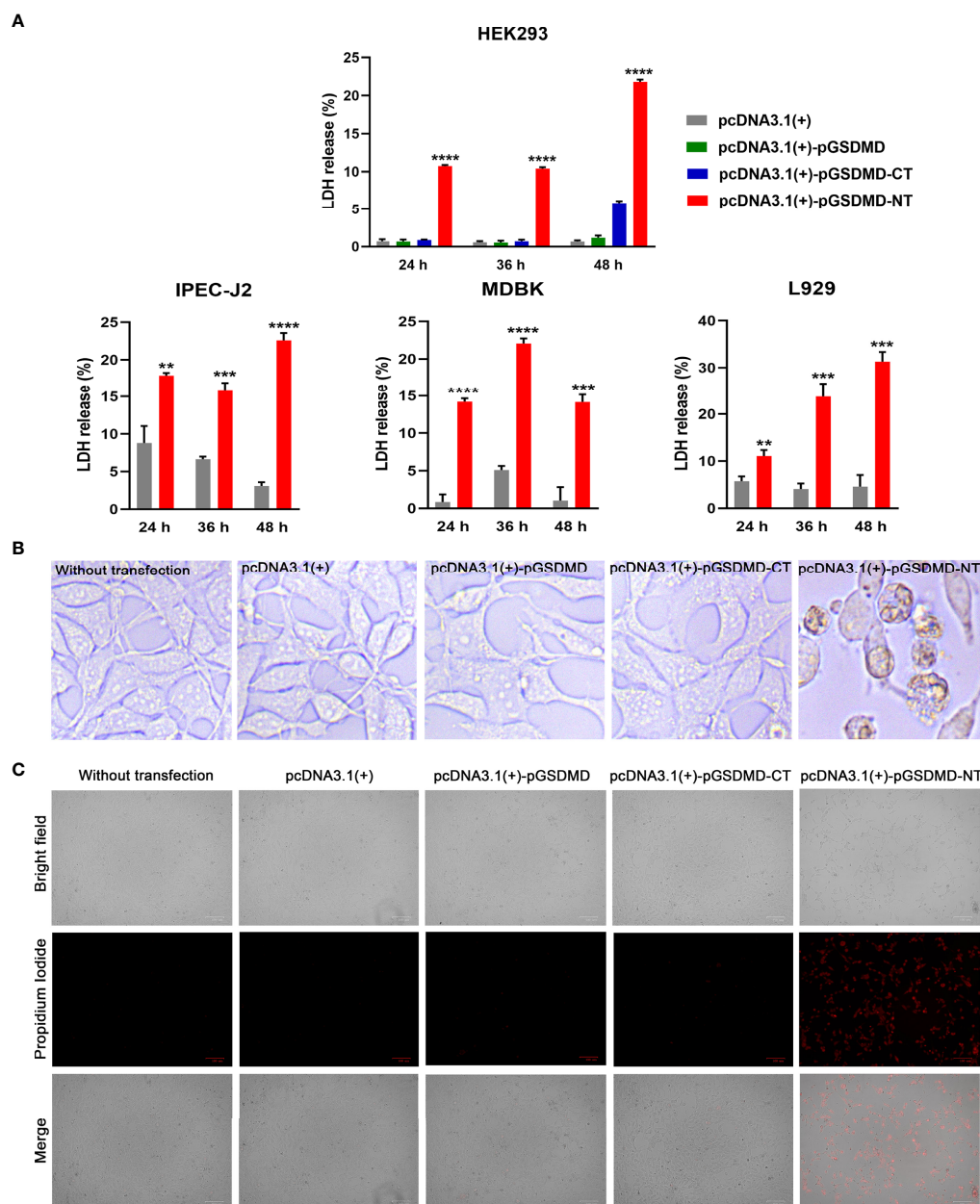


**FIGURE 6** | pGSDMD-NT caused cell membrane damage. **(A)** IPEC-J2, HEK293, L929 and MDBK cells were transfected with pcDNA3.1(+)-pGSDMD, pcDNA3.1(+)-pGSDMD-CT, pcDNA3.1(+)-pGSDMD-NT, or pcDNA3.1(+). The release of LDH was determined at 24, 36 and 48 h. Values are the means of triplicates and shown as means  $\pm$  SD. \*\* $p < 0.01$ , \*\*\* $p < 0.001$ , \*\*\*\* $p < 0.0001$ . **(B)** The representative pictures of the HEK293 cells transfected with pcDNA3.1(+)-pGSDMD, pcDNA3.1(+)-pGSDMD-CT, pcDNA3.1(+)-pGSDMD-NT, or pcDNA3.1(+) at 24 h after the transfection. **(C)** The transfected HEK293 cells were stained with PI and observed under an inverted fluorescence microscope.

humans and mice (8, 25), we speculated that pcaspase-1 activation and pGSDMD cleavage are closely related.

To determine the ability of pcaspase-1 to cleave pGSDMD in the cell-free system, we prepared active rpcaspase-1 in a prokaryotic expression system. Previous reports presented two strategies to obtain active human and mouse caspase-1 in the *E. coli* expression system. The first one is to purify the recombinantly expressed caspase-1 p20 and p10 subunits in *E. coli* cells under denaturing

condition and then dilute the mixture of p10 and p20 to allow them to refold and assemble into active rcaspase-1 (26). We have tried this strategy, but pcaspase-1 p10 failed to express in *E. coli* cells. The other strategy is to express the full-length rcaspase-1 in *E. coli* cells. Active rcaspase-1 can be obtained after the self-activation process (27). In the current study, His-rpcaspase-1, rpcaspase-1-His, and  $\Delta$ rpcaspase-1-His were expressed in *E. coli* (Figure 2). The results showed that active rpcaspase-1 was only obtained from the

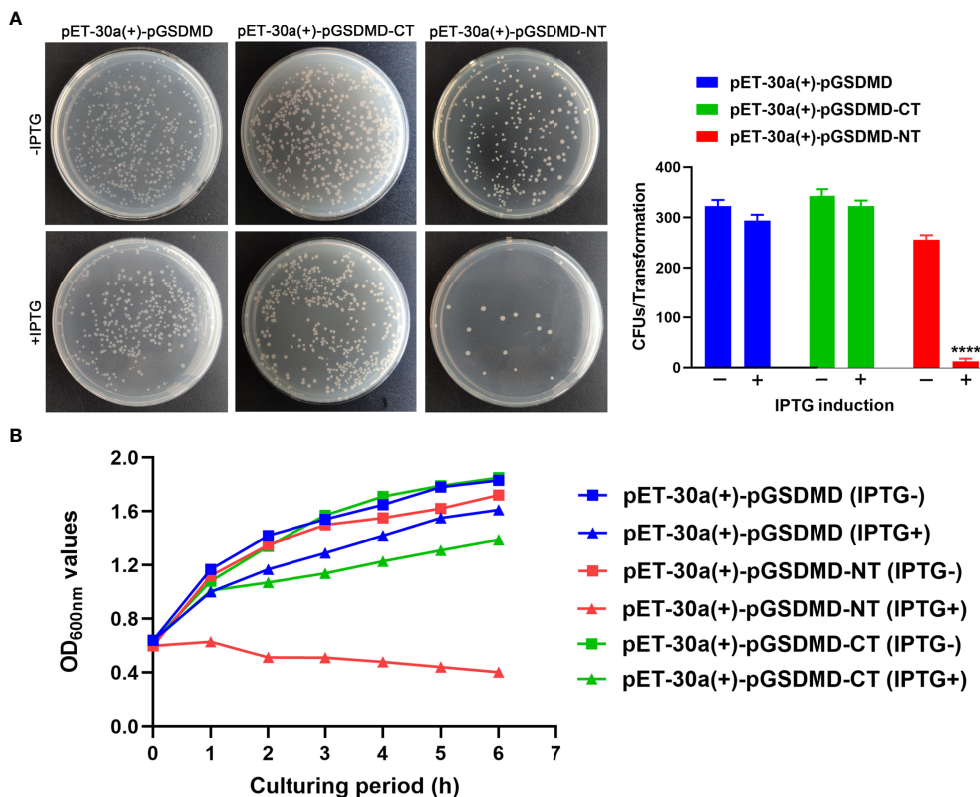


**FIGURE 7** | rpGSDMD-NT exhibits bactericidal activity. **(A)** *E. coli* that can express His-rpGSDMD, His-rpGSDMD-NT (1–279 residues) and His-rpGSDMD-CT (280–489 residues) grown on the plates in the presence or absence of IPTG for 12 h. Left panel shows the representative pictures of the plates. The number of colonies on the plates were counted and statistically calculated (right panel). Values are the means of triplicates and shown as means  $\pm$  SD. \*\*\*\* $p < 0.0001$ . **(B)** The OD<sub>600nm</sub> values of the liquid cultures of *E. coli* transformants expressing His-rpGSDMD, His-rpGSDMD-NT and His-rpGSDMD-CT.

His-rpcaspase-1 transformant. In addition, the fused-His tag at the amino-terminal domain of His-rpcaspase-1 was removed along with the prodomain during the self-activation process (the recombinant protein cannot be recognized by anti-His tag antibody; data not shown). A previous study demonstrated that the recombinantly expressed mouse caspase-1 with carboxyl-terminal fused His-tag and with or without prodomain could be autoprocessed into p10 and p20 subunits (27). Silkworm (*Bombyx mori*) caspase-1 and oyster (*Crassostrea gigas*) caspase-1 can also be autoprocessed in the prokaryotic expression system (28). Our results showed that rpcaspase-1-His could not be fully autoprocessed and that  $\Delta$ rpcaspase-1-His was expressed as an inclusion body. Although removal of the prodomain in rpcaspase-1-His was observed (the protein in the rpcaspase-1-His sample that can be recognized by the anti-rpcaspase-1 antibodies has the same molecular weight as  $\Delta$ rpcaspase-1-His), the separation of p20 and p10 subunits failed (Figure 2). The results indicated that a carboxyl-terminal fused oligopeptide significantly affected the auto processing of rpcaspase-1. For the above reasons, the *E. coli* lysate expressing the His-rpcaspase-1 was used as the source of active rpcaspase-1 without purification. The cleavage of His-rpGSDMD by His-rpcaspase-1 could therefore be determined by Western blot assay but not SDS-PAGE.

Previous studies have shown that GSDMD is a substrate of caspase-1 in humans and mice (8, 29). In the current study, we found that caspase-1 is capable of cleaving pGSDMD in the cell-free system and HEK293 cells (Figure 3). In addition, the caspase inhibitors can abolish the pGSDMD cleavage by caspase-1 (Figure 4), indicating that the enzymatic activity of caspase-1 is critical to its ability to cleave pGSDMD. These results reveal the relationship between the pcaspase-1 activation and pGSDMD cleavage that we observed in the intestinal tissue of the ETEC-challenged piglet (Figure 1).

The caspase-1 cleavage sites in human and murine GSDMDs are <sub>272</sub>FLTD|G<sub>276</sub> and <sub>273</sub>LLSD|G<sub>277</sub>, respectively (8). A previous work speculated that pGSDMD 1–279aa is the N-terminal fragment of pGSDMD caused by caspase-1 cleavage (23). Analysis of the pGSDMD's primary structure showed that the amino acid composition around the 279aa position of the pGSDMD molecule is <sub>276</sub>FQSD|G<sub>280</sub> (Figure 5A). This motif is similar to the caspase-1 cleavage sites of human and murine GSDMDs. Considering that caspases cleave proteins and peptide C-terminal to aspartic acid residues (30), D279 in the <sub>276</sub>FQSD|G<sub>280</sub> motif of the pGSDMD molecule was mutated to an alanine to verify the role of this motif in the pGSDMD cleavage by pcaspase-1 in the current study. The cleavage assay in cell-free system showed

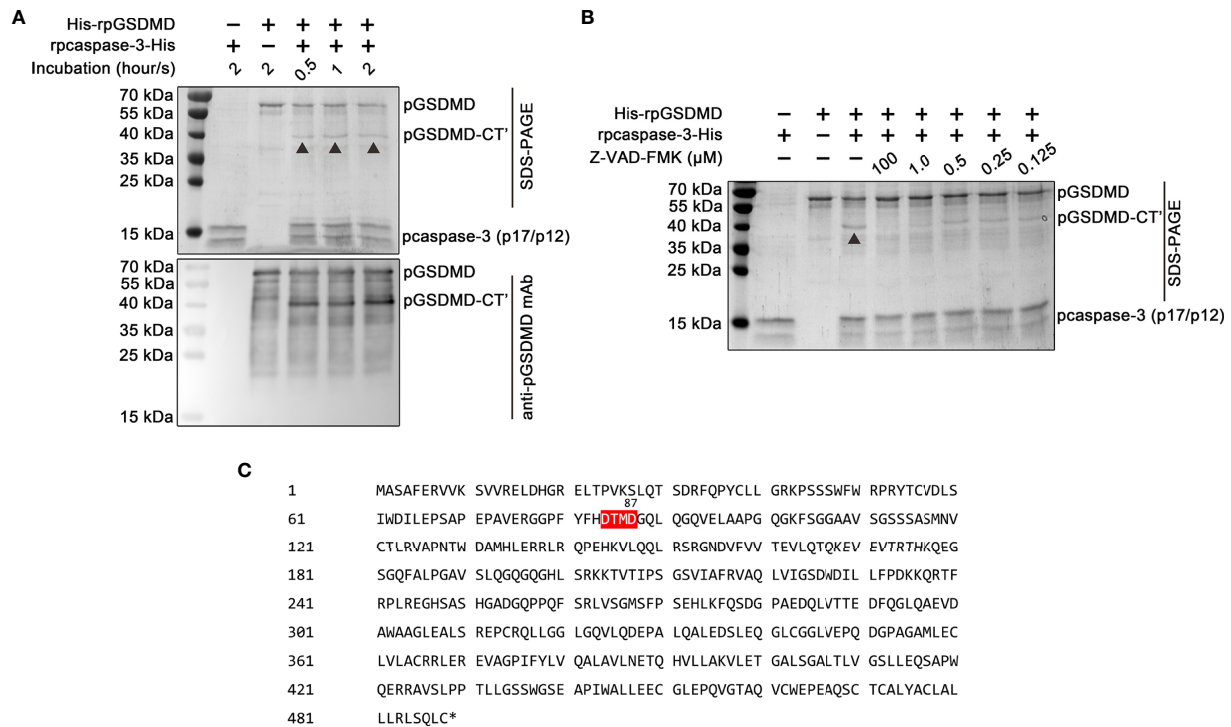


**FIGURE 8** | Cleavage of His-rpGSDMD by rpcaspase-3-His. **(A)** Purified His-rpGSDMD was incubated with purified rpcaspase-3-His for 0.5, 1 and 2 h. The cleavage products of His-rpGSDMD were analyzed by SDS-PAGE and western blot assay. **(B)** The effect of Z-DEVD-FMK on rpcaspase-3-His mediated His-rpGSDMD cleavage. **(C)** The diagram of deduced cleavage site of pcaspase-3 in pGSDMD.

that the D279A mutation completely abolished the pGSDMD cleavage by pcaspase-1 (**Figure 5B**). This result indicates that D279 is essential for the pcaspase-1-mediated pGSDMD cleavage and the FQSD|G is a new amino acid composition pattern that can be recognized and cleaved by caspase-1.

The GSDMD cleavage caused the disassociation of GSDMD-NT and GSDMD-CT (8, 31, 32). Human and murine GSDMD-NT can punch holes in the cell membrane and trigger pyroptosis (33, 34). The current study found that the pGSDMD-NT can cause damage to the cell membrane. Overexpression of pGSDMD-NT led to increased LDH release and PI entry in the cells (**Figure 6**). However, the immune staining result of a previous study showed that the overexpressed pGSDMD 1-277aa mainly aggregates into spots in the cells but is not located on the cell membrane (23). The exact mechanism of pGSDMD-NT to destroy the cell membrane's integrity is therefore worthy of further study. The pGSDMD-NT killed the *E. coli* Rosetta (DE3)<sup>TM</sup> rapidly when the former was expressed in the bacteria cells (**Figure 7**). This result does not exceed the expectation, because human and murine GSDMD-NT (33, 35) and pGSDMD 1-277aa (23) exhibited bactericidal activity in such system. However, our result regarding the lack of bactericidal activity of full-length pGSDMD (**Figure 7**) is inconsistent with the result of the previous study (23). This difference may be attributed to the different *E. coli* competent cells used in the two studies or the difference in the recombinant protein induction conditions.

Notably, pcaspase-3 was able to cleave pGSDMD *in vitro*, which is consistent with previous studies in humans and mice (24, 36). This result indicates that pcaspase-3 may also play roles in regulating pGSDMD-mediated pyroptosis.

In conclusion, our study shows that pGSDMD can be cleaved by pcaspase-1 and the NT domain of pGSDMD can cause damage in cell membrane and lead to pyroptosis-like cell death. Our study provides significant information about the mechanism of pyroptosis in porcine cells.

## DATA AVAILABILITY STATEMENT

The original contributions presented in the study are included in the article/supplementary material. Further inquiries can be directed to the corresponding authors.

## AUTHOR CONTRIBUTIONS

WZ designed the experiments, analyzed the results, supervised the work, and drafted the manuscript. YS performed most of the experiments and drafted the manuscript. JS prepared the mouse anti-porcine GSDMD monoclonal antibody. MW prepared active pcaspase-3 protein. BM and JW supervised the work. All authors read and approved the final version of the manuscript.

## FUNDING

This work was supported by the University Nursing Program for Young Scholars with Creative Talents in Heilongjiang Province,

grant number UNPYSCT-2017019 and “Academic Backbone” Project of Northeast Agricultural University, grant number 17XG09.

## REFERENCES

- Shi J, Gao W, Shao F. Pyroptosis: Gasdermin-Mediated Programmed Necrotic Cell Death. *Trends Biochem Sci* (2017) 42:245–54. doi: 10.1016/j.tibs.2016.10.004
- Fisch D, Bando H, Clough B, Hornung V, Yamamoto M, Shenoy AR, et al. Human GBP1 Is a Microbe-Specific Gatekeeper of Macrophage Apoptosis and Pyroptosis. *EMBO J* (2019) 38:e100926. doi: 10.15252/embj
- Qu Y, Misaghi S, Newton K, Maltzman A, Izrael-Tomasevic A, Arnott D, et al. NLRP3 Recruitment by NLR4 During Salmonella Infection. *J Exp Med* (2016) 213:877–85. doi: 10.1084/jem.20132234
- Galloway NL, Doitsh G, Monroe KM, Yang Z, Munoz-Arias I, Levy DN, et al. Cell-to-Cell Transmission of HIV-1 Is Required to Trigger Pyroptotic Death of Lymphoid-Tissue-Derived CD4 T Cells. *Cell Rep* (2015) 12:1555–63. doi: 10.1016/j.celrep.2015.08.011
- Zhao W, Yang H, Lyu L, Zhang J, Xu Q, Jiang N, et al. GSDMD, an Executor of Pyroptosis, is Involved in IL-1 $\beta$  Secretion in *Aspergillus fumigatus* Keratitis. *Exp Eye Res* (2021) 202:108375. doi: 10.1016/j.exer
- Zhang R, Chen J, Mao L, Guo Y, Hao Y, Deng Y, et al. Nobiletin Triggers Reactive Oxygen Species-Mediated Pyroptosis Through Regulating Autophagy in Ovarian Cancer Cells. *J Agric Food Chem* (2020) 68:1326–36. doi: 10.1021/acs.jafc.9b07908
- Wang L, Li K, Lin X, Yao Z, Wang S, Xiong X, et al. Metformin Induces Human Esophageal Carcinoma Cell Pyroptosis by Targeting the Mir-497/PELP1 Axis. *Cancer Lett* (2019) 450:22–31. doi: 10.1016/j.canlet.2019.02.014
- Shi J, Zhao Y, Wang K, Shi X, Wang Y, Huang H, et al. Cleavage of GSDMD by Inflammatory Caspases Determines Pyroptotic Cell Death. *Nature* (2015) 526:660–5. doi: 10.1038/nature15514
- Kayagaki N, Stowe IB, Lee BL, O'Rourke K, Anderson K, Warming S, et al. Caspase-11 Cleaves Gasdermin D for non-Canonical Inflammasome Signalling. *Nature* (2015) 526:666–71. doi: 10.1038/nature15541
- Kovacs SB, Miao EA. Gasdermins: Effectors of Pyroptosis. *Trends Cell Biol* (2017) 27:673–84. doi: 10.1016/j.tcb.2017.05.005
- Feng S, Fox D, Man SM. Mechanisms of Gasdermin Family Members in Inflammasome Signaling and Cell Death. *J Mol Biol* (2018) 430:3068–80. doi: 10.1016/j.jmb.2018.07.002
- Jiang S, Zhou Z, Sun Y, Zhang T, Sun L. Coral Gasdermin Triggers Pyroptosis. *Sci Immunol* (2020) 5:eabd2591. doi: 10.1126/sciimmunol.abd2591
- Orning P, Weng D, Starheim K, Ratner D, Best Z, Lee B, et al. Pathogen Blockade of TAK1 Triggers Caspase-8-Dependent Cleavage of Gasdermin D and Cell Death. *Science* (2018) 362:1064–9. doi: 10.1126/science
- Sarhan J, Liu BC, Muendlein HI, Li P, Nilson R, Tang AY, et al. Caspase-8 Induces Cleavage of Gasdermin D to Elicit Pyroptosis During *Yersinia* Infection. *Proc Natl Acad Sci USA* (2018) 115:E10888–97. doi: 10.1073/pnas.1809548115
- Xia S, Hollingsworth LT, Wu H. Mechanism and Regulation of Gasdermin-Mediated Cell Death. *Cold Spring Harb Perspect Biol* (2020) 12:a036400. doi: 10.1101/cshperspect.a036400
- Gaidt MM, Hornung V. Pore Formation by GSDMD Is the Effector Mechanism of Pyroptosis. *EMBO J* (2016) 35:2167–9. doi: 10.15252/embj.201695415
- Martins RP, Collado-Romero M, Martinez-Gomariz M, Carvajal A, Gil C, Lucena C, et al. Proteomic Analysis of Porcine Mesenteric Lymph-Nodes After *Salmonella* Typhimurium Infection. *J Proteomics* (2012) 75:4457–70. doi: 10.1016/j.jprot.2012.03.045
- Shan C, Miao S, Liu C, Zhang B, Zhao W, Wang H, et al. Induction of Macrophage Pyroptosis-Related Factors by Pathogenic *E. coli* High Pathogenicity Island (HPI) in Yunnan Saba Pigs. *BMC Vet Res* (2021) 17:114. doi: 10.1186/s12917-021-02824-x
- Yuan J, Zhu M, Deng S, Fan S, Xu H, Liao J, et al. Classical Swine Fever Virus Induces Pyroptosis in the Peripheral Lymphoid Organs of Infected Pigs. *Virus Res* (2018) 250:37–42. doi: 10.1016/j.virusres.2018.04.004
- Fan S, Yuan J, Deng S, Chen Y, Xie B, Wu K, et al. Activation of Interleukin-1 $\beta$  Release by the Classical Swine Fever Virus is Dependent on the NLRP3 Inflammasome, Which Affects Virus Growth in Monocytes. *Front Cell Infect Microbiol* (2018) 8:225. doi: 10.3389/fcimb.2018.00225
- Wei G, Luo S, Wu W, Hu J, Zhou R. Activation of Interleukin-1 $\beta$  Release and Pyroptosis by Transmissible Gastroenteritis Virus Is Dependent on the NOD-Like Receptor Protein 3 Inflammasome in Porcine Intestinal Epithelial Cell Line. *Viral Immunol* (2021) 34:401–9. doi: 10.1089/vim.2020.0227
- Song J, Wang K, Ma B, Wang J, Zhang W. Preparation of Rabbit Polyclonal Antibody Against Porcine Gasdermin D Protein and Determination of the Expression of Gasdermin D in Cultured Cells and Porcine Tissues. *Protein Expr Purif* (2021) 187:105945. doi: 10.1016/j.pep.2021.105945
- Wen W, Li X, Wang H, Zhao Q, Yin M, Liu W, et al. Seneca Valley Virus 3C Protease Induces Pyroptosis by Directly Cleaving Porcine Gasdermin D. *J Immunol* (2021) 207:189–99. doi: 10.4049/jimmunol.2001030
- Taabazuung CY, Okondo MC, Bachovchin DA. Pyroptosis and Apoptosis Pathways Engage in Bidirectional Crosstalk in Monocytes and Macrophages. *Cell Chem Biol* (2017) 24:507–14. doi: 10.1016/j.chembiol.2017.03.009
- Lu F, Lan Z, Xin Z, He C, Guo Z, Xia X, et al. Emerging Insights Into Molecular Mechanisms Underlying Pyroptosis and Functions of Inflammasomes in Diseases. *J Cell Physiol* (2020) 235:3207–21. doi: 10.1002/jcp
- Roschitzki-Voser H, Schroeder T, Lenherr ED, Frolich F, Schweizer A, Donepudi M, et al. Human Caspases In Vitro: Expression, Purification and Kinetic Characterization. *Protein Expr Purif* (2012) 84:236–46. doi: 10.1016/j.pep.2012.05.009
- Ramirez M, Poreba M, Snipas SJ, Groborz K, Drag M, Salvesen GS. Extensive Peptide and Natural Protein Substrate Screens Reveal That Mouse Caspase-11 has Much Narrower Substrate Specificity Than Caspase-1. *J Biol Chem* (2018) 293:7058–67. doi: 10.1074/jbc.RA117.001329
- Lu G, Yu Z, Lu M, Liu D, Wang F, Wu Y, et al. The Self-Activation and LPS Binding Activity of Executioner Caspase-1 in Oyster *Crassostrea gigas*. *Dev Comp Immunol* (2017) 77:330–9. doi: 10.1016/j.dci.2017.09.002
- Ramos-Junior ES, Morandini AC. Gasdermin: A New Player to the Inflammasome Game. *BioMed J* (2017) 40:313–6. doi: 10.1016/j.bj.2017.10.002
- Lien S, Pastor R, Sutherland D, Lowman HB. A Substrate-Phage Approach for Investigating Caspase Specificity. *Protein J* (2004) 23:413–25. doi: 10.1023/b:jopc.0000039555.92058.51
- Liu Z, Wang C, Yang J, Zhou B, Yang R, Ramachandran R, et al. Crystal Structures of the Full-Length Murine and Human Gasdermin D Reveal Mechanisms of Autoinhibition, Lipid Binding, and Oligomerization. *Immunity* (2019) 51:43–9. doi: 10.1016/j.immuni.2019.04.017
- Liu Z, Wang C, Rathkey JK, Yang J, Dubay GR, Abbott DW, et al. Structures of the Gasdermin D C-Terminal Domains Reveal Mechanisms of Autoinhibition. *Structure* (2018) 26:778–84. doi: 10.1016/j.str.2018.03.002
- Liu X, Zhang Z, Ruan J, Pan Y, Magupalli VG, Wu H, et al. Inflammasome-Activated Gasdermin D Causes Pyroptosis by Forming Membrane Pores. *Nature* (2016) 535:153–8. doi: 10.1038/nature18629
- Ding J, Wang K, Liu W, She Y, Sun Q, Shi J, et al. Pore-Forming Activity and Structural Autoinhibition of the Gasdermin Family. *Nature* (2016) 535:111–6. doi: 10.1038/nature18590
- Kuang S, Zheng J, Yang H, Li S, Duan S, Shen Y, et al. Structure Insight of GSDMD Reveals the Basis of GSDMD Autoinhibition in Cell Pyroptosis. *Proc Natl Acad Sci USA* (2017) 114:10642–7. doi: 10.1073/pnas
- Rogers C, Fernandes-Alnemri T, Mayes L, Alnemri D, Cingolani G, Alnemri ES. Cleavage of DFNA5 by Caspase-3 During Apoptosis Mediates Progression to Secondary Necrotic/Pyroptotic Cell Death. *Nat Commun* (2017) 8:14128. doi: 10.1038/ncomms14128

**Conflict of Interest:** The authors declare that the research was conducted in the absence of any commercial or financial relationships that could be construed as a potential conflict of interest.

**Publisher's Note:** All claims expressed in this article are solely those of the authors and do not necessarily represent those of their affiliated organizations, or those of the publisher, the editors and the reviewers. Any product that may be evaluated in

this article, or claim that may be made by its manufacturer, is not guaranteed or endorsed by the publisher.

Copyright © 2022 Song, Song, Wang, Wang, Ma and Zhang. This is an open-access article distributed under the terms of the Creative Commons Attribution License

(CC BY). The use, distribution or reproduction in other forums is permitted, provided the original author(s) and the copyright owner(s) are credited and that the original publication in this journal is cited, in accordance with accepted academic practice. No use, distribution or reproduction is permitted which does not comply with these terms.